ACS APPLIED MATERIALS & INTERFACES

Research Article

www.acsami.org

Solution-Processed Ultrasensitive Polymer Photodetectors with High External Quantum Efficiency and Detectivity

Xilan Liu, Hangxing Wang, Tingbin Yang, Wei Zhang, and Xiong Gong*

Department of Polymer Engineering, College of Polymer Science and Polymer Engineering, The University of Akron, Akron, Ohio 44325, United States

ABSTRACT: Operating at room temperature, polymer photodetectors (PDs) with external quantum efficiency approximately 80%, detectivity over 10^{13} Jones, linear dynamic range over 120 dB, and dark current a few decades of nA/cm^2 were demonstrated. All these performance parameters were achieved by combined treatment of active layer with solvent vapor annealing and of polymer PDs with postproduction thermal annealing. These high performance parameters demonstrated that polymer PDs is comparable to or better than inorganic counterparts.

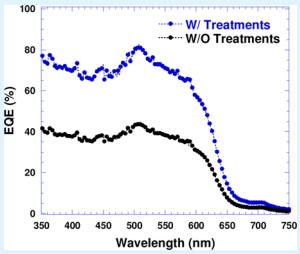

KEYWORDS: *semiconducting polymer, photodetectors, external quantum efficiency, detectivity, dark current, solvent and thermal annealing*

INTRODUCTION

In the last two decades, polymer electronic and optoelectronic devices, such as light-emitting diodes, field effect transistors, solar cells, and photodetectors (PDs) have been extensively investigated owing to their potential of being fabricated on flexible and lightweight substrates using low-cost and high-throughput printing techniques.[1−3] Polymer PDs have attracted much attention because of a variety of promising applications in optical sensing at room temperature.[4−8] Particularly, with the discovery of ultrafast photoinduced charge transfer from semiconducting polymers to buckminsterfullerene and its derivatives,[9] sensitive and fast temporal response polymer PDs have been demonstrated.[10−16]

The operation principles of polymer PDs are similar to those of polymer solar cells. It rests on the employment of photoactive layers that are best known as bulk heterojunction (BHJ). These systems are prepared by the composite of the electron donors (D, semiconducting polymers) and the electron acceptors (A, fullerenes and its derivatives), in which undergo consecutive processes of exciton generation, exciton dissociation, charge transfer and transport under illumination. The photocurrent density (J_{ph}) of polymer solar cells and polymer PDs depends on the intensity of light illuminated on the devices and the magnitude of external quantum efficiency (EQE). Regarding polymer PDs, an additional important device performance parameter is the detectivity (D), which relies on both J_{ph} and dark current density (J_d).[11] The spatial distribution of the separated phases of D and A in the active layer greatly affects J_{ph} and J_d, and an ideal morphology has been described as an interpenetrating network for efficient charge transport and less recombination.[17] Therefore, modification of morphology has been crucial and a key strategy in the optimization of device performance. At present, organic PDs with high D (more than 1×10^{10} Jones (1 Jones = 1 cm $H^{1/2}$/W)) have been demonstrated through controlled film morphology and by utilization of multilayer device architecture, however, the EQE was only a few percents.[10,12−16,18] For example, Forrest's group has demonstrated the organic PDs with D over 10^{10} Jones, nevertheless, the EQE was only 6.5%.[18] Polymer PDs with D over 10^{13} Jones has been demonstrated, but the EQE under zero bias was less than 10%.[11] In general, the EQE of polymer PDs and other organic PDs with spectral response at wavelength (λ) less than 800 nm is around 40%; and the EQE at $\lambda >$ 800 nm is only a few percent.[10−16,18] These values are much lower than those of inorganic counterparts.[19,20] Hence, polymer PDs with both high EQE and D have to be developed for its applications.

In this paper, we report solution-processed polymer PDs with approximately 80% of EQE, over 1×10^{13} Jones of D, the magnitude of nA/cm^2 of J_d and over 120 dB of linear dynamic range. All these performance parameters were achieved by combined treatment of polymer PDs with solvent vapor annealing and post production annealing.

EXPERIMENTAL SECTION

Materials. Poly(3-hexylthiophene) (P3HT) was purchased from Rieke Metals Inc. and (6,6)-phenyl-C_{61}-butyric acid methyl ester (PCBM) was provided by 1-Material Inc. used without further purification.

Device Fabrication and Characterization. Polymer PDs were fabricated on ITO (indium tin oxide) glass in the glovebox with nitrogen atmospheres. The active layer, composed of P3HT blended with PCBM (1:0.8 by weight), was cast from 2 wt % ortho-dichlorobenzene (o-DCB) solution followed with thermally annealing at 80 °C for 30 min. P3HT:PCBM layer with thickness ranged from 60 to 310 nm were obtained by tuning the speed of spin-casting. The anode, metal Al with thickness exceeding 200 nm, was thermally

Received: May 7, 2012
Accepted: June 15, 2012
Published: June 15, 2012

Table 1. Performance of Polymer Photodetectors

thickness[a] (nm)	J_d (A/cm^2)	J_{ph}[b] (A/cm^2)	EQE[c] (%)	R[d] (mA/W)	D[e] (Jones)
60	3.48×10^{-7}	9.03×10^{-5}	70	282	6.8×10^{11}
130	2.43×10^{-8}	8.65×10^{-5}	67	270	2.5×10^{12}
190	7.09×10^{-9}	6.50×10^{-5}	50	205	4.0×10^{12}
210	1.52×10^{-9}	5.84×10^{-5}	45	182	8.3×10^{12}
310	1.42×10^{-9}	4.32×10^{-5}	33	135	6.3×10^{12}

[a]Thickness of active layer. [b]Photocurrent measured at λ = 500 nm with an light intensity of 0.32 mW/cm^2 and at bias of −0.5 V. [c]EQE measured at λ = 500 nm. [d]Responsivity at λ = 500 nm. [e]The detectivity at λ = 500 nm and at bias of −0.5 V.

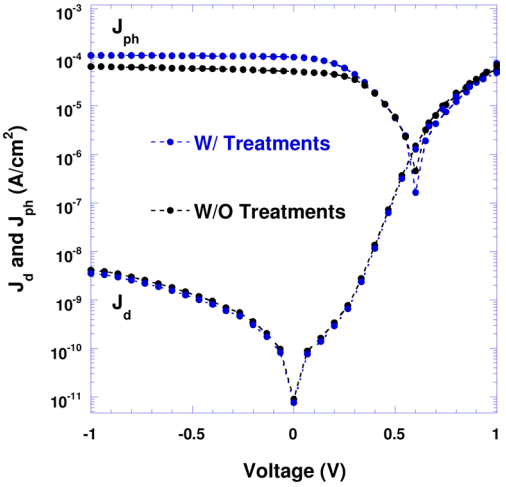

Figure 1. current-density versus voltage (J–V) characteristics of polymer PDs measured in the dark and under illumination (λ = 500 nm) with light intensity of 0.32 mW/cm^2.

deposited onto the top of polymer active layer. The active device area was 4.5 mm^2.

In order to optimize device performance, solvent-vapor annealing treatment[21] and postproduction thermal annealing treatment[22] were carried out. The solvent-vapor annealing treatment was exposing the fresh P3HT:PCBM active layer to saturated o-DCB solvent vapor at room temperature and atmosphere pressure in a closed jar for 10 min before 30-min thermal annealing at 80 °C. Postproduction treatment was that the final devices were thermally annealed at 150 °C for 10 min in the nitrogen atmospheres.

The current density versus voltage (J–V) characteristics was measured using a Keithley 2400 Source Measure Unit. The photocurrent of polymer PDs was characterized using a Newport Air Mass 1.5 Global (AM1.5G) full spectrum solar simulator at the wavelength of 500 nm with the light intensity of 0.32 mW/cm^2. The EQE was measured under short-circuit conditions and reverse bias using the lock-in amplifier technique.

Film Characterization. The surface morphologies of the active layer with and without o-DCB vapor treatment were characterized by tapping-mode atomic force microscopy (AFM) (Digital Instrument).

RESULTS AND DISCUSSION

Table 1 summarizes device performance parameters of polymer PDs with different thickness of active layer. As the active layer was about 60 nm, polymer PDs exhibited both high EQE and responsivity (R, a ratio of photocurrent to incident-light intensity) but poor D; as the active layer was about 310 nm, polymer PDs showed both poor EQE and R but a relatively high D. The best D and moderate EQE and R were observed from polymer PDs with the thickness of active layer about 210 nm. These data indicated that device performance (EQE, R, and D) of polymer PDs were active layer thickness dependent.

Further optimization of polymer PDs was carried out on the devices with a thickness of about 210 nm. The J–V characteristics of polymer PDs with and without combined treatment are shown in Figure 1. In the dark, polymer PDs showed a rectification ratio more than 1×10^4 at ±1 V, indicating the formation of well-made diodes. The J_d observed from polymer PDs with and without combined treatments were nearly identical. The J_d were smaller than 40 nA/cm^2 under the bias from 0 V to −1 V. These J_d were significantly lower than those from inorganic PDs.[20] Under the illumination of monochromatic light at λ = 500 nm, polymer PDs showed J_{ph} was more than 4 orders of magnitude higher than J_d at the reversed bias. This indicated that efficient exciton dissociation and ultrafast photoinduced charge transfer occurred among the P3HT:PCBM BHJ composite.[9,23] Moreover, it was observed that J_{ph} from polymer PDs with combined treatments was

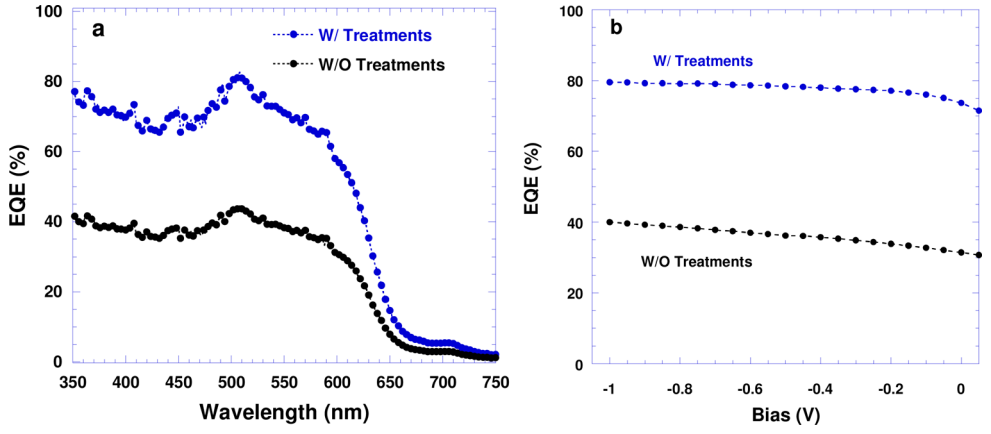

Figure 2. (a) External quantum efficiency under −0.5 V bias of polymer PDs versus light wavelengths; (b) external quantum efficiency of polymer PDs at λ = 500 nm versus bias voltage.

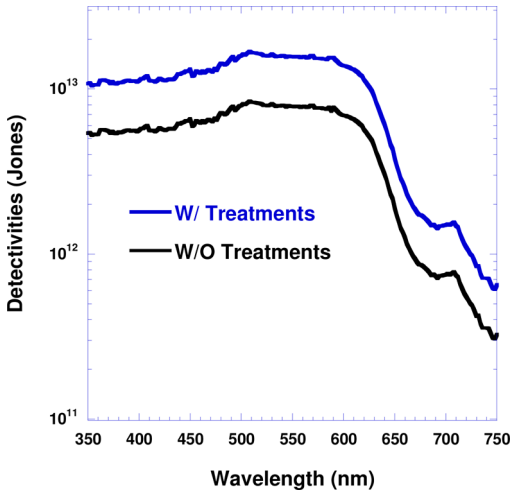

Figure 3. Detectivities at bias of −0.5 V for polymer photodetectors with and without combined treatments.

approximately twice larger than those without any treatment. This result demonstrated that J_{ph} of polymer PDs was enhanced by both solvent-vapor annealing treatment and postproduction thermal annealing treatment.

EQE spectra of polymer PDs are presented in Figure 2a, b, respectively. The EQE under reversed bias of −0.5 V from polymer PDs with combined treatments were nearly twice as high as those without any treatment over the entire spectra. And the EQE values were persistent under the reverse bias from 0 V to −1.0 V. This observation was consistent with the enhanced J_{ph} from polymer PDs with combined treatments. Under the bias of −1.0 V, EQE of polymer PDs at λ = 500 nm was 79.5% electron per photon. Accordingly, the R was calculated to be 320 mA/W. These are the highest values reported in the literature so far.

The performance was also evaluated by detectivity, one of the most important figures of merits (FOM) used for evaluating the performance of PDs. Projected detectivity, D*, described by eq 1, was used to estimate the signal-to-noise ratio of polymer PDs.[11]

$$D^* = (J^*_{ph}/L_{light})/(2qJ_d)^{1/2} \quad (1)$$

where L_{light} is the incident light intensity and q is the electron charge. The plots of D^* at bias of −0.5 V versus wavelengths for polymer PDs are shown in Figure 3. The D^* was more than 1×10^{11} Jones for whole visible spectral range, whereas 350−650 nm was the premium detection range with D^* from polymer PDs with the combined treatments more than 1×10^{13} Jones. These results are comparable to those observed from inorganic counterparts.

Previous studies in polymer solar cells indicated that the phase separation of crystalline P3HT aggregates and PCBM domains was a complex exothermic process which could be affected by solvent vapor annealing and postproduction thermal annealing.[24] Both techniques concentrated on improving the nanoscale lateral phase separation of the two-component system. Solvent-vapor annealing method was used to control the polymer nanomorphology through the solvent removal speed.

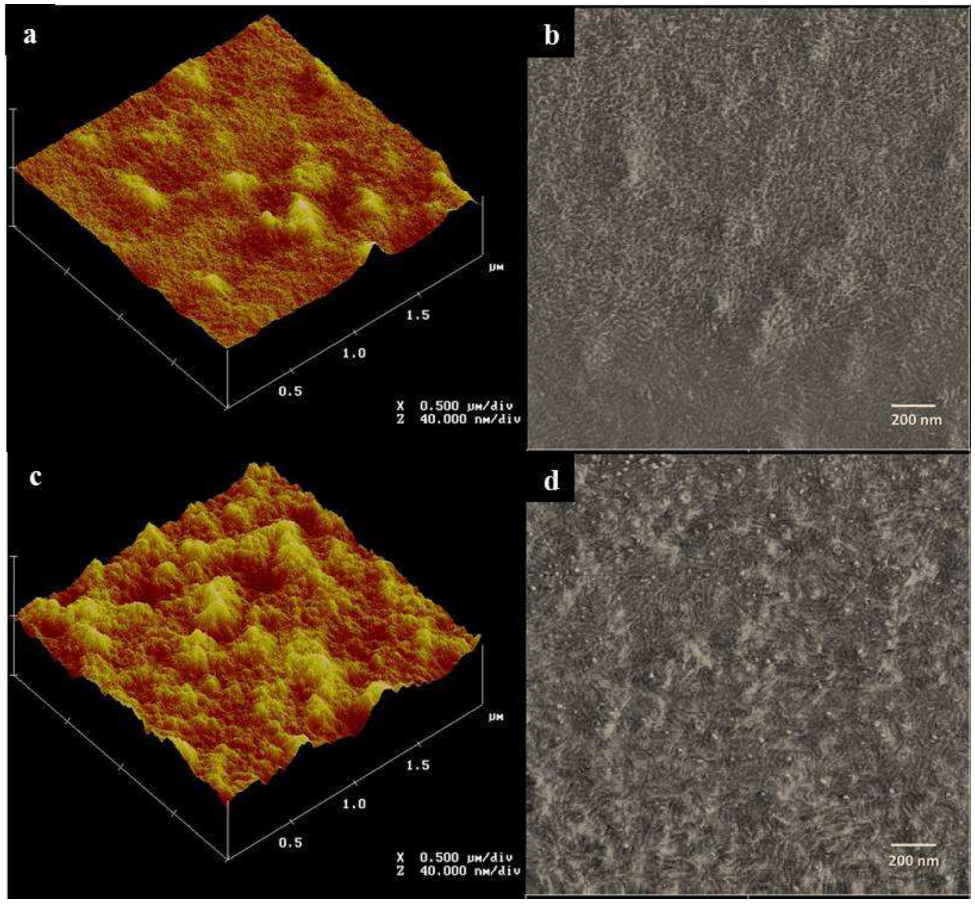

Figure 4. Tapping mode AFM images of P3HT:PCBM film (a, b) without solvent-vapor annealing and (c, d) with solvent-vapor annealing.

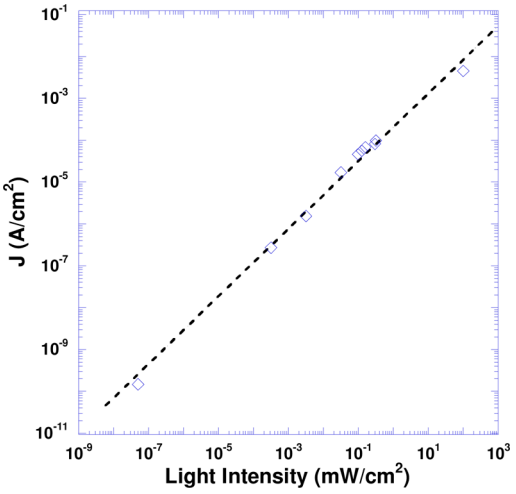

Figure 5. Linear dynamic range of the polymer photodetector.

By slowing down the film-growth rate, P3HT molecules can be self-organized into more ordered structure where interlaid distance and nanoscale crystallinity of polymer chains would be higher.[21,25−27] As a result, the hole mobility and optical absorption of P3HT were enhanced. In order to confirm this hypothesis, AFM was carried out to study the film morphology. Figure 4 displayed the tapping mode AFM images of P3HT:PCBM films without (Figures 4a,b) and with solvent-vapor annealing (Figures 4c,d). The AFM phase images in Figures 4b,d showed the emergence of crystalline nanofibrils and a higher contrast of separated phases upon the solvent-vapor treatment. These indicated that more ordered packing of polymer and domains with higher purity of the rich component. As a result, enhanced charge mobility in the spontaneously separated phases could be expected. In addition, a rougher surface for film with solvent-vapor annealing (Figure 4c, $R_{rms} \approx$ 3 nm) was induced as compared to that without the treatment (Figure 4a; $R_{rms} \approx 1.8$ nm). This slight change would facilitate a strong interaction and more contact areas between the active layer and top electrode.[22]

Postproduction thermal annealing has been widely used for improving the performance of P3HT:PCBM solar cells.[22,28−31] X-ray diffraction (XRD) studies have demonstrated that a lifted intensity of thiophene ring $\pi-\pi$ stacking peak and an emerging peak resulting from side-chain interdigitations appeared after the solar cells were treated at 150 °C for 5 min.[22] These enhanced packing of molecules and/or nanoscale crystallinity would certainly enhance the mobility of charge carriers. Moreover, AFM and transmission electron microscopy (TEM) studies also demonstrated that more complete phase separation and the formation of bicontinuous interpenetrating networks from the active layer occurred by the postproduction treatment.[22] Therefore, better charge carrier transport was promoted from the BHJ composite to the corresponding electrodes, resulting in enhanced photocurrent. Accordingly, EQE of polymer PDs were dramatically enhanced by the combined solvent-vapor annealing treatment and postproduction thermal annealing treatment.

Linear dynamic range (LDR) is another FOM used for evaluation of PDs. LDR is given by LDR=20Log(J^*_{ph}/J_d), in which J_{ph}^* is the photocurrent measured at light intensity of 1 mW/cm^2.[11] The LDR for polymer PDs with combined treatments was shown in Figure 5. It can be seen that polymer PDs can response linearly to the light intensity until 100 mW/cm^2, and the LDR was greater than 120 dB, which is even higher than that from Si PDs.[11] These results are the best up-to-date and are comparable to or better than those of inorganic silicon based PDs.

CONCLUSION

Solution-processed polymer photodetectors based on P3HT:PCBM BHJ composite were demonstrated with spectral response from 350 to 750 nm. By combined solvent-vapor annealing treatment of active layer and postproduction thermal annealing treatment of formed cells, polymer photodetectors with external quantum efficiency approximately 80%, detectivity greater than 1×10^{13} Jones, linear dynamic range over 120 dB, and dark current a few decades nA/cm^2 were obtained. These high performance parameters demonstrated that polymer photodetectors are comparable to or better than inorganic counterparts.

AUTHOR INFORMATION

Corresponding Author

*E-mail: xgong@uakron.edu; fax: (330) 972 2339.

Notes

The authors declare no competing financial interest.

ACKNOWLEDGMENTS

The authors thank the University of Akron and 3M Company for financial support.

REFERENCES

(1) Coakley, K. M.; McGehee, M. D. *Chem. Mater.* **2004**, *16*, 4533−4542.
(2) Hadziioannow, G.; Malliaras, C. G. In *Semiconducting Polymers*; Wiley-VCH: Weinheim, Germany, 2007, Vol. *1* & Vol. *2*, p1.
(3) Heeger, A. J.; Sariciftchi, N. S.; Namdas, E. B. In *Semiconducting and Metallic Polymers*; Oxford University Press: New York, 2010, p31.
(4) Ettenberg, M. *Adv. Imaging* **2005**, *20*, 29−32.
(5) Konstantatos, G.; Howard, I.; Fischer, A.; Hoogland, S.; Clifford, J.; Klem, E.; Levina, L.; Sargent, E. H. *Nature* **2006**, *442*, 180−183.
(6) Sargent, E. H. *Adv. Mater.* **2005**, *17*, 515−522.
(7) Kim, S.; Lim, Y. T.; Soltesz, E. G.; De Grand, A. M.; Lee, J.; Nakayama, A.; Parker, J. A.; Mihaljevic, T.; Laurence, R. G.; Dor, D. M.; Cohn, L. H.; Bawendi, M. G.; Frangioni, J. V. *Nat. Biotechnol.* **2004**, *22*, 93−7.
(8) McDonald, S. A.; Konstantatos, G.; Zhang, S.; Cyr, P. W.; Klem, E. J. D.; Levina, L.; Sargent, E. H. *Nat. Mater.* **2005**, *4*, 138−142.
(9) Sariciftci, N. S.; Simliowitz, L.; Wudl, F.; Heeger, A. J. *Science* **1992**, *258*, 1474−1476.
(10) Yu, G.; Pakbaz, K.; Heeger, A. J. *Appl. Phys. Lett.* **1994**, *64* (25), 3422−3424.
(11) Gong, X.; Tong, M.; Xia, Y.; Cai, W.; Moon, J. S.; Cao, Y.; Yu, G..; Shieh, C.-L.; Nilsso, B.; Heeger, A. J. *Science* **2009**, *325*, 1665−1667.
(12) Schilinsky, P.; Waldauf, C.; Barabec, C. J. *Appl. Phys. Lett.* **2002**, *81*, 3885−3887.
(13) O'Brien, G. A.; Quinn, A. J.; Tanner, D. A.; Redmond, G. *Adv. Mater.* **2006**, *18*, 2379−2383.
(14) Yao, Y.; Liang, Y.; Shrotriya, V.; Xiao, S.; Yu, L.; Yang, Y. *Adv. Mater.* **2007**, *19*, 3979−3983.
(15) Chen, E.-C.; Chang, C.-Y.; Shieh, J.-T.; Tseng, S.-R.; Meng, H.-F.; Hsu, C.-S.; Horng, S.-F. *Appl. Phys. Lett.* **2010**, *96*, 043507.
(16) Keivanidis, P. E.; Ho, P. K. H.; Friend, R. H.; Greenham, N. C. *Adv. Funct. Mater.* **2010**, *20*, 3895−3903.
(17) Guenes, S.; Neugebauer, H.; Sariciftci, N. S. *Chem. Rev.* **2007**, *107*, 1324−1338.

(18) Zimmerman, J. D.; Diev, V. V.; Hanson, K.; Lunt, R. R.; Yu, E. K.; Thompson, M. E.; Forrest, S. R. *Adv. Mater.* **2010**, *22*, 2780−2783.
(19) Sze, S. M.; Ng, K. K. In *Physics of Semiconductor Devices*, third ed.; John Wiley-Interscience: New York, 2007, p672.
(20) Jha, A. R. In *Infrared Technology: Applications to Electro-optics, Photonic Devices and Sensors*; Wiley-Interscience: New York, 2000, p133.
(21) Zhao, Y.; Xie, Z.; Qu, Y.; Geng, Y.; Wang, L. *Appl. Phys. Lett.* **2007**, *90*, 043504.
(22) Ma, W.; Yang, C.; Gong, X.; Lee, K.; Heeger, A. J. *Adv. Funct. Mater.* **2005**, *15*, 1617−1622.
(23) Blom, P. W. M.; Mihailetchi, V. D.; Koster, L. J. A.; Markov, D. E. *Adv. Mater.* **2007**, *19*, 1551−1566.
(24) Chen, L.-M.; Hong, Z.; Li, G.; Yang, Y. *Adv. Mater.* **2009**, *21*, 1434−1449.
(25) Yang, H.; Shin, T. J.; Yang, L.; Cho, K.; Ryu, C. Y.; Bao, Z. *Adv. Funct. Mater.* **2005**, *15*, 671−676.
(26) Chu, C. W.; Yang, H.; Hou, W. J.; Huang, J.; Li, G.; Yang, Y. *Appl. Phys. Lett.* **2008**, *92*, 103306.
(27) Li, G.; Yao, Y.; Yang, H.; Shrotriya, V.; Yang, G.; Yang, Y. *Adv. Funct. Mater.* **2007**, *17*, 1636−1644.
(28) Dittmer, J. J.; Marseglia, E. A.; Friend, R. H. *Adv. Mater.* **2000**, *12*, 1270−1274.
(29) Camaioni, N.; Ridolfi, G.; Meceli, G. C.; Possamai, G.; Maggini, M. *Adv. Mater.* **2002**, *14*, 1735−1738.
(30) Padinger, F.; Rittberger, R. S.; Sariciftci, N. S. *Adv. Funct. Mater.* **2003**, *13*, 85−88.
(31) Li, G.; Shrotriya, V.; Yao, Y.; Yang, Y. *J. Appl. Phys.* **2005**, *98*, 043704.